Volume 44 | Number 31 | 21 August 2015 | Pages 13763–14180

# Dalton Transactions

An international journal of inorganic chemistry

www.rsc.org/dalton

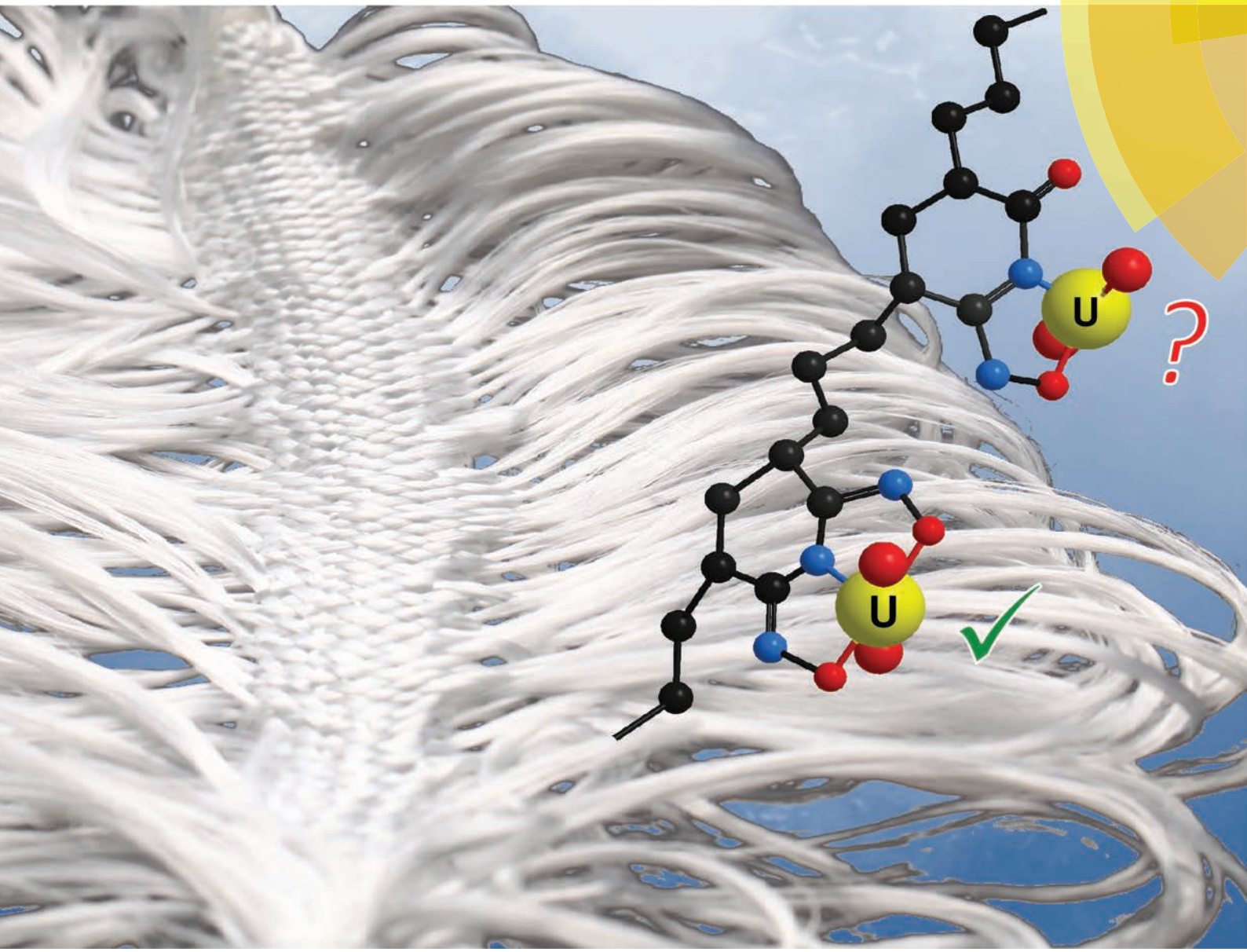


ISSN 1477-9226

ROYAL SOCIETY OF CHEMISTRY

PAPER

Linfeng Rao *et al.*

Complexation of uranium(VI) with glutarimidoxioxime: thermodynamic and computational studies

Dalton Transactions

PAPER

Cite this: *Dalton Trans.*, 2015, **44**, 13835

# Complexation of uranium(VI) with glutarimidoxioxime: thermodynamic and computational studies†

Francesco Endrizzi,[a] Andrea Melchior,[b] Marilena Tolazzi[b] and Linfeng Rao*[a]

The complex formation between a cyclic ligand glutarimidoxioxime (denoted as $HL^{III}$ in this paper) and $UO_2^{2+}$ is studied by potentiometry and microcalorimetry. Glutarimidoxioxime ($HL^{III}$), together with glutarimidedioxime ($H_2L^{I}$) and glutardiamidoxime ($H_2L^{II}$), belongs to a family of amidoxime derivatives with prospective applications as binding agents for the recovery of uranium from seawater. An optimized procedure of synthesis that leads to the preparation of glutarimidoxioxime in the absence of other amidoxime byproducts is described in this paper. Speciation models based on the thermodynamic results from this study indicate that, compared with $H_2L^{I}$ and $H_2L^{II}$, $HL^{III}$ forms a much weaker complex with $UO_2^{2+}$, $UO_2(L^{III})^{+}$, and cannot effectively compete with the hydrolysis equilibria of $UO_2^{2+}$ under neutral or alkaline conditions. DFT computations, taking into account the solvation by including discrete hydration water molecules and bulk solvent effects, were performed to evaluate the structures and energies of the possible isomers of $UO_2(L^{III})^{+}$. Differing from the tridentate or $\eta^2$-coordination modes previously found in the U(VI) complexes with amidoxime-related ligands, a bidentate mode, involving the oxygen of the oxime group and the nitrogen of the imino group, is found to be the most probable mode in $UO_2(L^{III})^{+}$. The bidentate coordination mode seems to be stabilized by the formation of a hydrogen bond between the carbonyl group of $HL^{III}$ and a water molecule in the hydration sphere of $UO_2^{2+}$.

Received 20th January 2015,
Accepted 17th April 2015

DOI: 10.1039/c5dt00261c

www.rsc.org/dalton

## Introduction

Recovery of uranium from seawater has recently become a topic of interest in scientific research, following an increased demand for the use of uranium in nuclear power plants and the quest for more sustainable alternatives to terrestrial mining for the supply of this nuclear fuel.[1,2] In this regard, the prospective recovery of uranium naturally existing in seawater is currently being investigated for technical feasibility and cost assessment. In fact, although seawater contains uranium in very low concentrations (about 3 ppb), the overall amount of dissolved uranium is expected to be 4.5 billion tons, that is 1000 times more than the amount of uranium expected to exist in terrestrial ores, to date. Given the very low concentration of uranium in seawater, its extraction is therefore a challenging task. In addition, it is known that uranium exists in seawater in its hexavalent state, forming a very stable anionic triscarbonato complex, $[(UO_2)(CO_3)_3]^{4-}$.[3] More recent studies[4,5] suggest that this complex is further stabilized by the formation of ternary complexes with calcium and magnesium that are in high concentrations in seawater. Therefore, to extract uranium effectively from seawater, the extracting agents must be able to form strong complex(es) with uranium by means of displacing both the carbonate and the calcium/magnesium ions from the coordination sphere of U(VI). Among the different methods that were studied in the last three decades, amidoxime-based sorption systems have shown the most promise.[3,6,7] In these systems, polyethylene fibers are copolymerized with polyacrylonitrile sidechains by a radiation-induced grafting process (Scheme 1a). Nitrile groups are then converted to amidoxime derivatives by reacting with hydroxylamine in ethanol/water solution. Depending on the reaction conditions (in particular, the molar ratio of hydroxylamine to nitrile and the reaction temperature), a few different amidoxime derivatives could be obtained as shown in Scheme 1a. The derivatives, ranging from the closed-ring glutarimidedioxime moiety (blue, Scheme 1a), to the open-ring amidoxime moiety (green, Scheme 1a), and the closed-ring glutarimidoxioxime moiety (red, Scheme 1a), could have very different binding abil-

[a]*Chemical Sciences Division, Lawrence Berkeley National Laboratory, 1 Cyclotron Rd., Berkeley, California 94720, USA. E-mail: lrao@lbl.gov; Tel: +1 5104865427; Fax: +1 5104865596*

[b]*Dipartimento Chimica Fisica e Ambiente, Università di Udine, Via Cotonificio 108, 33100 Udine, Italy*

†Electronic supplementary information (ESI) available: NMR data, analytical data for titration experiments, and computational software reference. See DOI: 10.1039/c5dt00261c

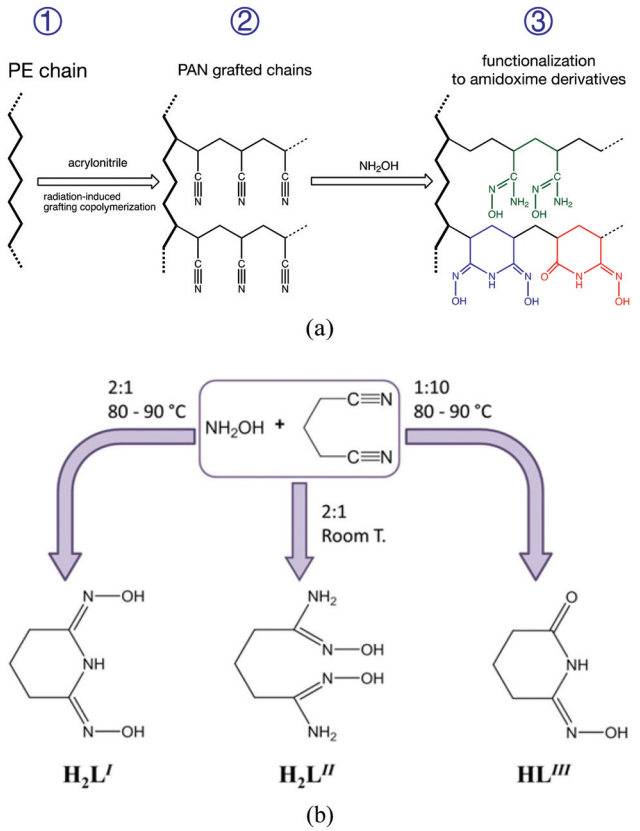


**Scheme 1** (a) Functionalization of polyacrylonitrile (PAN) sidechains with amidoxime derivatives; (b) optimized experimental conditions for the synthesis of three amidoxime derivatives (glutarimidedioxime, $H_2L^I$; glutardiamidoxime, $H_2L^{II}$; glutarimidoxioxime, $HL^{III}$).

ities with U(VI), affecting the overall sorption ability of the sorbent for the extraction of uranium from seawater. To improve the efficiency of uranium extraction, it is necessary to systematically evaluate the binding ability of each of the possible configurations, so that the conditions of the grafting/reaction process could be optimized to achieve the maximum yield of the configuration with the highest binding ability towards uranium.

To help the development of more efficient amidoxime-based sorbents, three amidoxime-related small molecules that represent the three moieties shown in Scheme 1a have been prepared and studied. By selecting different experimental conditions, each of the three ligands, including glutarimidedioxime ($H_2L^I$), glutardiamidoxime ($H_2L^{II}$), and glutarimidoxioxime ($HL^{III}$), were obtained in high yields, as shown in Scheme 1b. Thermodynamic and structural studies have been conducted for the complexation of U(VI) and other metal ions with $H_2L^I$ and $H_2L^{II}$.[8,9] Results showed that glutarimidedioxime ($H_2L^I$) and glutardiamidoxime ($H_2L^{II}$) both form strong complexes with uranyl in aqueous solution. In particular, the tridentate $H_2L^I$ ligand forms such strong complexes with U(VI) that it can effectively compete with carbonate for U(VI) under seawater conditions.

In the present study, thermodynamic measurements were conducted to quantify the binding ability of glutarimidoxioxime ($HL^{III}$), the third ligand in the series shown in Scheme 1b, towards U(VI). DFT calculations were performed to provide insight into the coordination mode in the U(VI)/$HL^{III}$ complex. Results from this study on $HL^{III}$, in conjunction with the previous results on $HL^I$ and $HL^{II}$, complete the systematic evaluation of the binding abilities of the possible configurations on the amidoxime-based sorbents, and help to optimize the process conditions to obtain the most efficient sorbent.

## Experimental

### Chemicals

All experiments were carried out at $T$ = 298.15 K and $I$ = 0.5 M NaCl (a concentration close to that in seawater). All solutions were prepared using MilliQ water, freshly boiled and cooled under an Ar stream to remove traces of dissolved carbon dioxide. NaCl was purchased from Sigma-Aldrich (pur. 99%), recrystallized twice from MilliQ water, and dried prior to use. Hydroxylamine (50% solution in water) and glutaronitrile (pur. >99%) were purchased from Sigma-Aldrich and used without further purification. Uranyl solutions were prepared by dilution of a standardized stock (0.251 M $UO_2^{2+}$, 0.221 M $HClO_4$). The uranium concentration in the stock solution was verified by fluorimetry according to known procedures.[10] The concentration of the free acid in the stock was assessed by potentiometric titrations, using a glass electrode and Gran's method to determine the equivalent point.

Glutarimidoxioxime ($HL^{III}$) was prepared by the reaction of glutaronitrile and hydroxylamine (10 : 1 molar ratio) in mixed ethanol/water solvent at 80–90 °C. This procedure is similar to that described for the preparation of glutarimidedioxime ($H_2L^I$) in the literature,[8] but differs in the molar ratio of the two reactants (see Scheme 1b). Using a large excess of glutaronitrile with respect to hydroxylamine helped to obtain $HL^{III}$ in high purity, while using lower ratios of glutaronitrile to hydroxylamine would result in the formation of significant amounts of $H_2L^I$. In detail, 9.40 grams (100 mmol) of glutaronitrile were added in 250 mL of a 60% (vol.) ethanol/water mixture and the solution was heated at 80 °C under stirring. Then, a solution of 0.70 g hydroxylamine (10 mmol) in 25 mL 60% ethanol/water was added dropwise under stirring. The reaction mixture was gently boiled under stirring for 5 days. The product was then concentrated by evaporation of the solvent under vacuum. The excess of unreacted glutaronitrile was removed by washing the product with successive small aliquots of cold MilliQ water ($T$ = 278.15 K). The product was finally washed with a few milliliters of cold ethanol ($T$ = 253.15 K) to remove any trace of byproducts, and dried under vacuum at room temperature for 24 h. The purity of the product was checked by $^1$H-NMR and $^{13}$C-NMR in DMSO-d$^6$ (the NMR data are provided in the ESI, Fig. S1†).

### Studies of the protonation of glutarimidoxioxime ($HL^{III}$)

$HL^{III}$ has two protonation sites, resulting in up to two successive protonation equilibria in aqueous solution, according to Scheme 2.

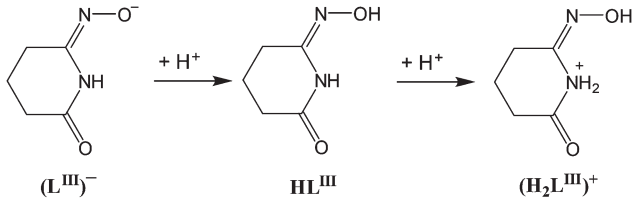


Scheme 2 Stepwise protonation of $HL^{III}$.

**Potentiometric experiments.** The ligand protonation was investigated by potentiometry, using a constant stream of argon in the cell to avoid the sorption of atmospheric $CO_2$, possibly occurring under alkaline conditions. A Metrohm Dosimat automatic burette (prec. ± 0.001 mL) was used to deliver the titrant in the cell solution. The electrode potential was collected with a Metrohm Potentiometer (prec. ± 0.1 mV) equipped with a combined glass electrode (Metrohm Unitrode). A series of experiments were carried out by titrating the cell solutions (16–20 mL, 6 to 16 mM $HL^{III}$, 0.01 M $H^+$) with 100 mM NaOH. To study the formation of $(H_2L^{III})^+$, an experiment was also performed by titrating a cell solution containing 6.0 mM $(L^{III})^-$ and an excess of $OH^-$ (1.7 mM) with a standardized solution of 0.5 M HCl (analytical data in the ESI, Table S1†).

Prior to the titration experiments, the electrode was thermostated at 298.15 K in an acidic solution with $I$ = 0.5 M (NaCl), until the electrode potential became stable within ±0.1 mV $h^{-1}$. The electrode was then calibrated, according to Nernst's law, by a standard acid/base titration to obtain the electrode parameters that were used to accurately relate the measured potentials with the free acidity in solution in subsequent titrations. The calibrations were carried out at the same temperature and ionic strength as those in the titration experiments.

Data collected from multiple titrations ($E$ in mV *vs.* $V_{add}$ in mL) were processed with the minimization software Hyperquad 2008.[11,12] The two protonation steps (shown in Scheme 2) were included in the model and the protonation constants were calculated. The data indicated that the second protonation step, occurring on the imino group leading to the formation of $(H_2L^{III})^+$, became significant only under highly acidic conditions (p[H] < 1.2).‡ Because the sensitivity of the glass electrode is significantly lower at such high acidity, the uncertainty of the second protonation constant calculated from potentiometry could be high. As a result, microcalorimetry, described in the next section, was approached as an independent technique to determine the second protonation constant as well as the enthalpies of protonation.

**Microcalorimetric experiments.** A TAM III isothermal microcalorimeter (TA Instruments) was used and calibrated according to the standard procedures described previously.[13,14] A series of five microcalorimetric titrations, carefully designed to alternatively maximize the formation of species including $(H_2L^{III})^+$, $HL^{III}$, and $(L^{III})^-$, were carried out. In a typical experiment, the cup was filled with 0.75 mL solution of $HL^{III}$ (3.9 to 19 mM) and titrated with 100 mM HCl or NaOH. To accurately determine the small protonation heat associated with the formation of $(H_2L^{III})^+$, two "reversed" titrations were also carried out, where the cup solution of 100 mM or 500 mM HCl was titrated with 19.0 mM $HL^{III}$ (analytical data in the ESI, Table S1†). The conditions of the reversed titrations maximized the formation of $(H_2L^{III})^+$. The observed heat at the $j$-th addition, $Q_{ex,j}$, was corrected by the heat of titrant dilution ($Q_{dil,j}$) that was measured in separate runs, to obtain the net reaction heat at the $j$-th point, $Q_{r,j} = Q_{ex,j} - Q_{dil,j}$. The calorimetric data from all titrations, in terms of the net reaction heat ($Q_{r,j}$ in mJ) as a function of the titrant volume ($V_{add}$ in μL) were processed with a least-squares minimization software Letagrop Kalle.[15]

### Studies of the complexation of $UO_2^{2+}$ with glutarimidoxioxime ($HL^{III}$)

Initially, both UV-Vis spectrophotometric and potentiometric titrations were used to investigate the formation of uranyl complexes with $HL^{III}$, using cup solutions containing 0.020 to 0.50 mM $UO_2^{2+}$, a 3.5–4 fold molar excess $HL^{III}$ (0.08 to 1.7 mM), and an initial p[H] = 2.0 that was titrated with 20.0 mM NaOH. These experiments were not successful because the precipitation of uranyl hydroxides was observed at the end of titrations (p[H] > 4.5), suggesting that the complexation of $UO_2^{2+}$ with $HL^{III}$ is too weak to effectively compete with the hydrolysis of $UO_2^{2+}$.

In order to overcome the precipitation of uranyl and to successfully study the formation of complexes with $HL^{III}$ by potentiometry, a series of competitive potentiometric experiments were designed, using ethylenediamine tetraacetic acid (EDTA) to stabilize U(VI) in solution and prevent the precipitation of U(VI) hydroxides. Moderate concentrations of EDTA were used in the titrations (molar ratio of [EDTA]/[U(VI)] ~ 0.5 to 1) so that the formation of the U(VI)/$HL^{III}$ complex was not overwhelmed by the U(VI)/EDTA complexes while, at the same time, the formation of the hydrolyzed U(VI) species was significantly reduced in the p[H] range 2.5–5.0. Multiple titrations were carried out with the 10–20 mL initial solutions (p[H] = 2.6) containing 0.4–0.5 mM $UO_2^{2+}$, 1.2–2.0 mM $HL^{III}$, and 0.2 mM EDTA, being titrated with 20.0 mM NaOH until a p[H] ~ 5.0 (analytical data in the ESI, Table S2†).

### DFT calculations

Density functional theory (DFT) calculations were carried out on the ligand and the complexes using the three-parameter hybrid functional B3LYP,[16,17] as this level of theory has been previously demonstrated to produce reliable structural and energetic results for actinide and lanthanide complexes.[18,19] The Stuttgart–Dresden small core potential[20] was employed for uranium because, in combination with the B3LYP functional, it has been demonstrated to generate computational results of reaction energies and vibrational frequencies of U(VI) complexes in good agreement with experimental data.[18] Other

‡ p[H] = −log[$H^+$].

elements were treated using the 6-31++G(d,p) Gaussian-type basis set. Solvent effect was taken into account by using the polarizable continuum model (PCM),[21] for which the cavity has been constructed using the UFF radii for the spheres centered on each atom of the solute.

Solvation can strongly affect the relative thermodynamic stabilities of reaction products when passing from the gas phase to solution.[22–25] In our case, to take into account the effects of metal de-solvation and complex hydration on the preferential coordination mode with $HL^{III}$, several $[UO_2(L^{III})\text{-}(H_2O)_n{\cdot}m(H_2O)]^+$ complexes ($n$ = 0, 3, and 4; $m$ = 0, 1, and 2; $n + m$ = 0–5) have been considered. Geometry optimizations were first carried out in a vacuum and produced true minimum structures as no imaginary frequencies were found. As far as the solvent effect on the energies is considered, a common practice is to use the gas-phase geometry and do the energy calculation in the presence of the polarizable continuum.[18,26–28] However, in this work, re-optimization of the complex geometries was performed, starting from the energy-minimized gas-phase structures. The re-optimization produced slightly different minima (no imaginary frequencies) with only very small changes in the geometries of the complex and reagent structures (with the exception of bond lengths in some species, *e.g.*, the species k and l discussed in a later section). Reaction energies were computed using the electronic energy for each reactant and product with the zero point energy and thermal corrections, which comprise the electronic, vibrational, rotational, and translational contributions to the internal energy. For the calculation of the reaction free energy in the solvent, the procedure proposed by Martin *et al.*[29] was adopted. This procedure has previously been applied to the study of complexation thermochemistry in aqueous solutions[18] and organic solvents.[26,28] This consists of the correction accounting for the reduction in translational entropy of the water molecule in the condensed phase by setting the pressure to 1354 atm (instead of 1 atm used as default) in the thermochemical analysis (the value derived from the liquid density of 997.02 kg $m^{-3}$ at 298 K). All calculations have been carried out using the Gaussian09 package.[30]

## Results and discussion

### Protonation of $HL^{III}$

The best fit of the potentiometric data (Fig. 1) was obtained with a model including two successive protonation constants: $\log \beta_{HL}$ = (10.82 ± 0.03) and $\log \beta_{H_2L}$ = (12.2 ± 0.1), according to Scheme 2.

Two representative microcalorimetric titrations are shown in Fig. 2. The data were fitted simultaneously for the protonation equilibrium constants and enthalpies. As shown in Fig. 2, very good fits were achieved. The first protonation constant obtained from calorimetry, $\log \beta_{HL}$(Cal.) = (10.85 ± 0.02), is essentially the same as that obtained by potentiometry (10.82 ± 0.03). The second protonation constant (from calorimetry), $\log \beta_{H_2L}$(Cal.) = (12.0 ± 0.1), overlaps that obtained by potentiometry within uncertainties (12.2 ± 0.1). In the calculation of the final enthalpies of protonation, we opted to use the protonation constants of (10.82 ± 0.03) and (12.0 ± 0.1), taking into consideration that the second protonation constant from potentiometry may be less certain due to the reduced

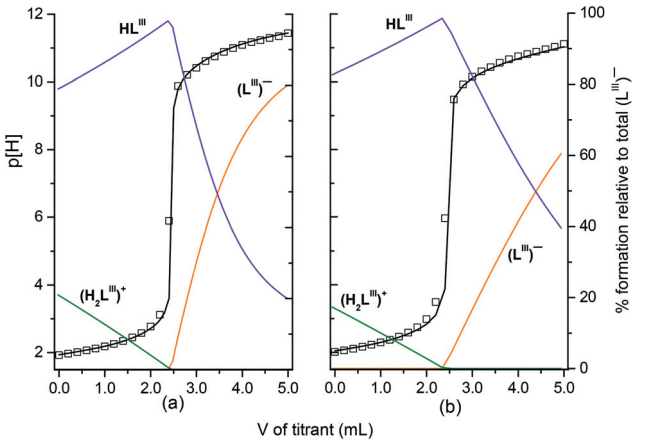


**Fig. 1** Potentiometric titrations of $HL^{III}$. Left axis: p[H] *vs.* $V_{add}$ (mL); right axis: percentage formation relative to total $HL^{III}$. (a): $C_H^0$ = 20.3, $C_L^0$ = 7.20 mM, $C_{OH}^{titr}$ = 101.6 mM; (b): $C_H^0$ = 27.7 mM, $C_L^0$ = 15.8 mM, $C_{OH}^{titr}$ = 101.6 mM. (Some points are omitted for clarity). The solid black curve is calculated by using the protonation constants in Table 1. Some points are omitted for clarity.

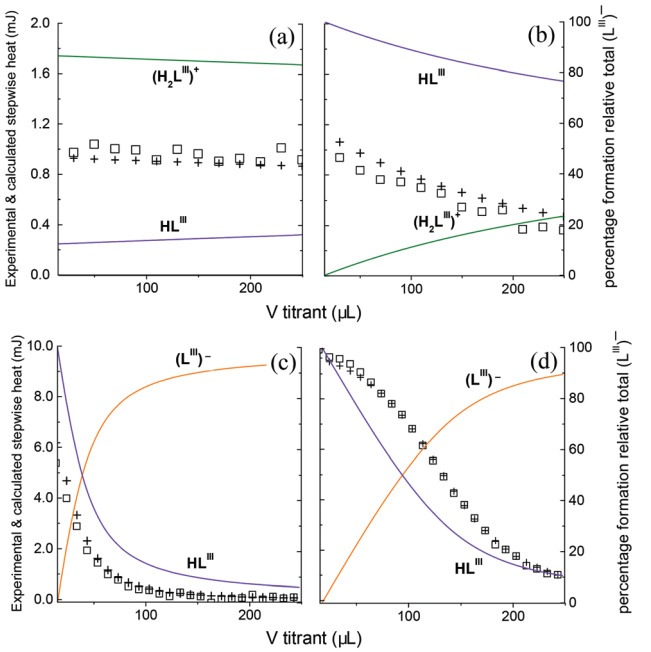


**Fig. 2** Microcalorimetric titrations of the protonation of glutarimidoxioxime ($HL^{III}$). Left axis: exp. (□) and cal. (+) stepwise heat $Q$ (mJ) *vs.* $V$ of titrant added (μL).; right axis: speciation of the ligand. Concentrations: (a) $C_H^0$ = 490 mM, $C_L^0$ = 0.251 mM, $C_{HL}^{titr}$ = 19.2 mM; (b) $C_{HL}^0$ = 19.2 mM, $C_H^{titr}$ = 99.9 mM; (c) $C_{HL}^0$ = 3.86 mM, $C_{OH}^{titr}$ = 101.6 mM; (d) $C_{HL}^0$ = 19.1 mM, $C_{OH}^{titr}$ = 101.6 mM. Some points are omitted for clarity.

Table 1 Thermodynamic data for the protonation and complexation of $HL^{III}$ with U(VI) at infinite dilution ($\log \beta^0$) and $I$ = 0.5 M ($\log \beta$). $T$ = 298.15 K. Data for pertinent reactions from the literature are also listed

| Reaction | $\log \beta^0 \pm \sigma$ | $\log \beta \pm \sigma$ (0.5 M NaCl) | $\Delta G \pm \sigma$ (kJ mol$^{-1}$) | $\Delta H \pm \sigma$ (kJ mol$^{-1}$) | $T\Delta S \pm \sigma$ (kJ mol$^{-1}$) | Ref. |
|---|---|---|---|---|---|---|
| **$H^+ + (L^{III})^- = HL^{III}$** | | **10.82 ± 0.03**[a] | **−61.77 ± 0.06** | **−35.91 ± 0.02** | **25.86 ± 0.06** | **p.w.** |
| **$2H^+ + (L^{III})^- = (H_2L^{III})^+$** | | **12.0 ± 0.1**[b] | **−68.5 ± 0.6** | **−42.03 ± 0.01** | **26.5 ± 0.6** | **p.w.** |
| **$H^+ + HL^{III} = (H_2L^{III})^+$** | | **1.2 ± 0.1** | **−6.9 ± 0.6** | **−6.12 ± 0.02** | **0.8 ± 0.6** | **p.w.** |
| **$UO_2^{2+} + (L^{III})^- = [(UO_2)L^{III}]^+$** | | **9.4 ± 0.6**[c] | | | | **p.w.** |
| $UO_2^{2+} + H_2O = [(UO_2)(OH)]^+ + H^+$ | −5.25 ± 0.24 | −5.65 ± 0.30 | | | | 31 |
| $3UO_2^{2+} + 5H_2O = [(UO_2)_3(OH)_5]^+ + 5H^+$ | −15.55 ± 0.12 | −16.9 ± 0.2 | | | | 31 |
| $UO_2^{2+} + edta^{4-} = [(UO_2)(edta)]^{2-}$ | 13.7 ± 0.2 | 11.3 ± 0.2 | | | | 32 |
| $UO_2^{2+} + H^+ + edta^{4-} = [(UO_2)(Hedta)]^-$ | 19.61 ± 0.10 | 16.53 ± 0.12 | | | | 32 |
| $H^+ + edta^{4-} = H(edta)^{3-}$ | 11.24 ± 0.03 | 10.12 ± 0.10 | | | | 32 |
| $2H^+ + edta^{4-} = H_2(edta)^{2-}$ | 18.04 ± 0.04 | 16.07 ± 0.11 | | | | 32 |
| $3H^+ + edta^{4-} = H_3(edta)^-$ | 21.19 ± 0.04 | 18.57 ± 0.11 | | | | 32 |
| $4H^+ + edta^{4-} = H_4(edta)(aq.)$ | 23.42 ± 0.06 | 20.35 ± 0.09 | | | | 32 |
| $H^+ + OH^- = H_2O$ | | 13.7004 ± 0.0003 | | −56.5 ± 0.1 | | 39, **p.w.** |

[a] Determined with potentiometry. [b] Determined with microcalorimetry. [c] The uncertainty of ±0.6 is actually 3 times the 1$\sigma$ value obtained from the calculation by HyperQuad. The uncertainty was enlarged to account for the propagation of the uncertainties for the pertinent reactions involved in the titration that was not taken into consideration by the HyperQuad program.

sensitivity of the electrode in strongly acidic solutions. Table 1 summarizes the values of the protonation constants and enthalpies of $HL^{III}$.

The protonation constants of $HL^{III}$ are compared in Table 2 with $H_2L^I$ and $H_2L^{II}$ that have been previously studied.[8,9] As shown in Scheme 1b, the three ligands, $HL^{III}$, $H_2L^I$, and $H_2L^{II}$ have two, three, and four protonation sites, respectively. For all three ligands, the first protonation equilibrium occurs on the oxime group and the protonation constants are similar (Table 2). The second protonation equilibria of $H_2L^I$ and $H_2L^{II}$ occur on the second oxime groups with the stepwise protonation constants close to the first one. In contrast, the second protonation of $HL^{III}$ occurs on the imino nitrogen, leading to the formation of a positively charged species $(H_2L^{III})^+$, and is characterized by a rather small stepwise protonation constant ($\log K$ = 1.2). This is in agreement with the small value of the third stepwise protonation constant of $H_2L^I$ ($\log K$ = 2.12) involving the protonation of its imino group.

The enthalpies of protonation shown in Table 2 also indicate that the protonation of the oxime group is highly exothermic, while the protonation of the imino group is much less exothermic. In particular, the enthalpies of protonation of $HL^{III}$ and $H_2L^I$ are very similar for the oxime group: $\Delta H_{HL^{III}}$ = −35.9 kJ mol$^{-1}$, $\Delta H_{H_2L^I}$ = −36.1 kJ mol$^{-1}$ and for the imino group: $\Delta H_{(H_2L^{III})^+}{}^{step}$ = −6.1 kJ mol$^{-1}$, $\Delta H_{(H_3L^I)^+}{}^{step}$ = −6.1 kJ mol$^{-1}$. The similar trends in the protonation constants and enthalpies of the three ligands are in line with the similarity in their structures.

## Complexation of U(VI) with $HL^{III}$, in comparison with $HL^I$ and $HL^{II}$

Fig. 3 shows the potentiometric titrations for the complexation of U(VI) with $HL^{III}$ using EDTA as a competing ligand. A number of speciation models were tried and the best fit of the experimental data was obtained with a model including the formation of a 1 : 1 complex $(UO_2L^{III})^+$ in the p[H] region of

Table 2 Thermodynamic data for the protonation and complexation of three amidoxime-related ligands ($I$ = 0.5 M NaCl, $T$ = 298.15 K)

| Ligand | Reaction | $\log \beta \pm \sigma$ | $\Delta H \pm \sigma$ (kJ mol$^{-1}$) | Ref. |
|---|---|---|---|---|
| **Glutarimidoxioxime ($HL^{III}$)** | **$H^+ + (L^{III})^- = HL^{III}$** | **10.82 ± 0.03** | **−35.91 ± 0.02** | **p.w.** |
| | **$2H^+ + (L^{III})^- = (H_2L^{III})^+$** | **12.0 ± 0.1** | **−42.03 ± 0.01** | **p.w.** |
| | **$H^+ + HL^{III} = (H_2L^{III})^+$** | **1.2 ± 0.1** | **−6.12 ± 0.02** | **p.w.** |
| | **$UO_2^{2+} + (L^{III})^- = [(UO_2)L^{III}]^+$** | **9.4 ± 0.6** | | **p.w.** |
| Glutardiamidoxime ($H_2L^{II}$) | $H^+ + (L^{II})^{2-} = (HL^{II})^-$ | 12.13 ± 0.12 | −52 ± 2 | 9 |
| | $2H^+ + (L^{II})^{2-} = H_2L^{II}$ | 24.19 ± 0.07 | −103 ± 3 | 9 |
| | $3H^+ + (L^{II})^{2-} = (H_3L^{II})^+$ | 29.98 ± 0.07 | −124 ± 6 | 9 |
| | $4H^+ + (L^{II})^{2-} = (H_4L^{II})^{2+}$ | 34.77 ± 0.07 | −151 ± 8 | 9 |
| | $UO_2^{2+} + (L^{II})^{2-} = (UO_2)L^{II}$ | 17.3 ± 0.3 | −49 ± 6 | 9 |
| Glutarimidedioxime ($H_2L^I$) | $H^+ + (L^I)^{2-} = (HL^I)^-$ | 12.06 ± 0.23 | −36.1 ± 0.5 | 8 |
| | $2H^+ + (L^I)^{2-} = H_2L^I$ | 22.76 ± 0.31 | −69.7 ± 0.9 | 8 |
| | $3H^+ + (L^I)^{2-} = (H_3L^I)^+$ | 24.88 ± 0.35 | −77 ± 6 | 8 |
| | $H^+ + H_2L^I = (H_3L^I)^+$ | 2.12 ± 0.47 | −7 ± 6 | 8 |
| | $UO_2^{2+} + (L^I)^{2-} = (UO_2)L^I$ | 17.8 ± 1.1 | −59 ± 8 | 8 |

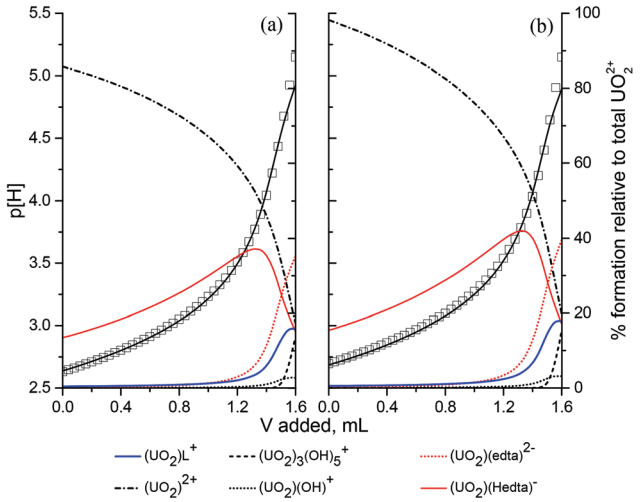


**Fig. 3** Potentiometric titrations for the complexation of U(VI) with $HL^{III}$. Left axis: p[H], □ experimental, – calculated. The full black curve is calculated by using the protonation constants in Table 1. Right axis: speciation of U(VI). Conditions: (a) $C_U^0$ = 0.46 mM, $C_H^0$ = 4.82 mM, $C_L^0$ = 1.95 mM, $C_{edta}^0$ = 0.23 mM, $C_{OH}^{titr}$ = 20.0 mM; (b) $C_U^0$ = 0.41 mM, $C_H^0$ = 3.75 mM, $C_L^0$ = 1.21 mM, $C_{edta}^0$ = 0.21 mM, $C_{OH}^{titr}$ = 20.0 mM.

3–5, with $\log\beta_{11}$ = (9.4 ± 0.6) (Table 1). In the calculation, the equilibrium constants of $UO_2^{2+}$ hydrolysis, EDTA protonation, and $UO_2^{2+}$ complexation with EDTA, at $I$ = 0.5 M (NaCl) were all included (see Table 1). These constants at $I$ = 0.5 M (NaCl) were obtained from those at infinite dilution[31,32] by using the Specific Ion Interaction Theory.[33] The constants at infinite dilution and $I$ = 0.5 M (NaCl) are also listed in Table 1.

The data from this work indicate that only one weak 1 : 1 complex between U(VI) and $HL^{III}$ is formed, even at high ligand/uranium molar ratios (3 : 1 and 4 : 1 in Fig. 3). In contrast, a series of U(VI) complexes with different stoichiometries were observed for $HL^{I}$ and $HL^{II}$.[8,9] Besides, the complexation of $HL^{III}$ with U(VI) is obviously much weaker than that of $HL^{I}$ or $HL^{II}$. For the 1 : 1 complex with U(VI), the value of $\log\beta_{11}$ for $(UO_2L^{III})^+$ is (9.4 ± 0.6), about eight orders of magnitude lower than that for $UO_2L^{I}$ (17.8 ± 1.1) and $UO_2L^{II}$ (17.3 ± 0.3) (Table 2).

The substantially weaker binding ability of $HL^{III}$ than that of $HL^{I}$ toward U(VI) is probably due to the lower denticity of $HL^{III}$. Previous studies have demonstrated that the cyclic $H_2L^{I}$ (glutarimidedioxime, Scheme 1b) is a tridentate ligand and forms strong chelate complexes with $UO_2^{2+}$ using the two oxime groups and the imino nitrogen.[8,34,35] The chelate structure of the U(VI) complex with $H_2L^{I}$ is particularly stabilized by a large conjugated ligand moiety that resulted from the relocation of the protons on the oxime groups and the deprotonation of the imino nitrogen.[8] In contrast, the absence of a second oxime group in $HL^{III}$ makes it less likely to form the same conjugated moiety and bind U(VI) in a strong tridentate mode. Therefore, $HL^{III}$ probably binds U(VI) in a mono- or bi-dentate mode. Attempts to obtain crystal structures of the $(UO_2L^{III})^+$ complex in this work were not successful. However, postulations on the coordination modes in this complex could be made, based on the information in the literature on the U(VI) complexes with related amidoxime ligands.[34,36] Three possible coordination modes, including bi-dentate, mono-dentate, and $\eta^2$-coordination, could be suggested (Fig. 4). The mono-dentate and $\eta^2$-coordination modes have been observed in U(VI) complexes with ligands structurally similar to $HL^{III}$. For example, the 1 : 1 U(VI) complex with acetamidoxime (AO), structurally similar to $HL^{III}$, is shown to have stability ($\log\beta_{11}$ = 10.6)[36] similar to that of U(VI)/$HL^{III}$ from this work ($\log\beta_{11}$ = (9.4 ± 0.6), Table 2). Also, X-ray crystallographic analysis in the solid phase,[37,38] combined with more recent DFT calculations,[34] has shown that $\eta^2$-coordination exists in the U(VI)/AO complex, without the involvement of the –$NH_2$ group.

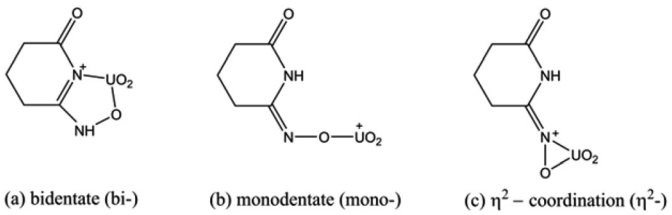


**Fig. 4** Possible coordination modes between $HL^{III}$ and $UO_2^{2+}$.

In the absence of the crystallographic data on the structure of the $(UO_2L^{III})^+$ complex, DFT calculations were performed in this work to provide insight into the coordination mode(s) and help explain the binding strength and thermodynamic trends in the complexation of $HL^{III}$ with U(VI).

## Coordination geometry

Several coordination modes in the $UO_2(L^{III})^+$ complex are possible, including bidentate chelation involving the oxime oxygen atom and the imino nitrogen atom (bi-), monodentate binding to the oxygen atom of the oxime group (mono-), and $\eta^2$-coordination to the N–O bond ($\eta^2$-) (Fig. 4).[34]

The geometries of different hydrated complexes $[UO_2L^{III}\text{-}(H_2O)_n{\cdot}m(H_2O)]^+$ ($n$ = 0, 3, 4; $m$ = 0, 1, 2; $n + m$ = 0–5) (structures a to l in Fig. 5) were first optimized in the gas phase. An increased number of water molecules has been included to evaluate the effect of uranyl hydration on the preferential coordination mode with $(L^{III})^-$. The bond distances of the structures in the gas phase are provided in Table S3 of the ESI.†

Then the structures were re-optimized in PCM water to take into account bulk solvation effects on the energy and structure of the reactants and products. Selected relevant bond distances for the complexes optimized in solution are summarized in Table 3.

In Table 4 are reported the $\Delta G$ values for reaction (1) for a–c and reaction (2) for d–l:

$$[UO_2]^{2+} + (L^{III})^- \rightarrow [UO_2L^{III}]^+ \quad (1)$$

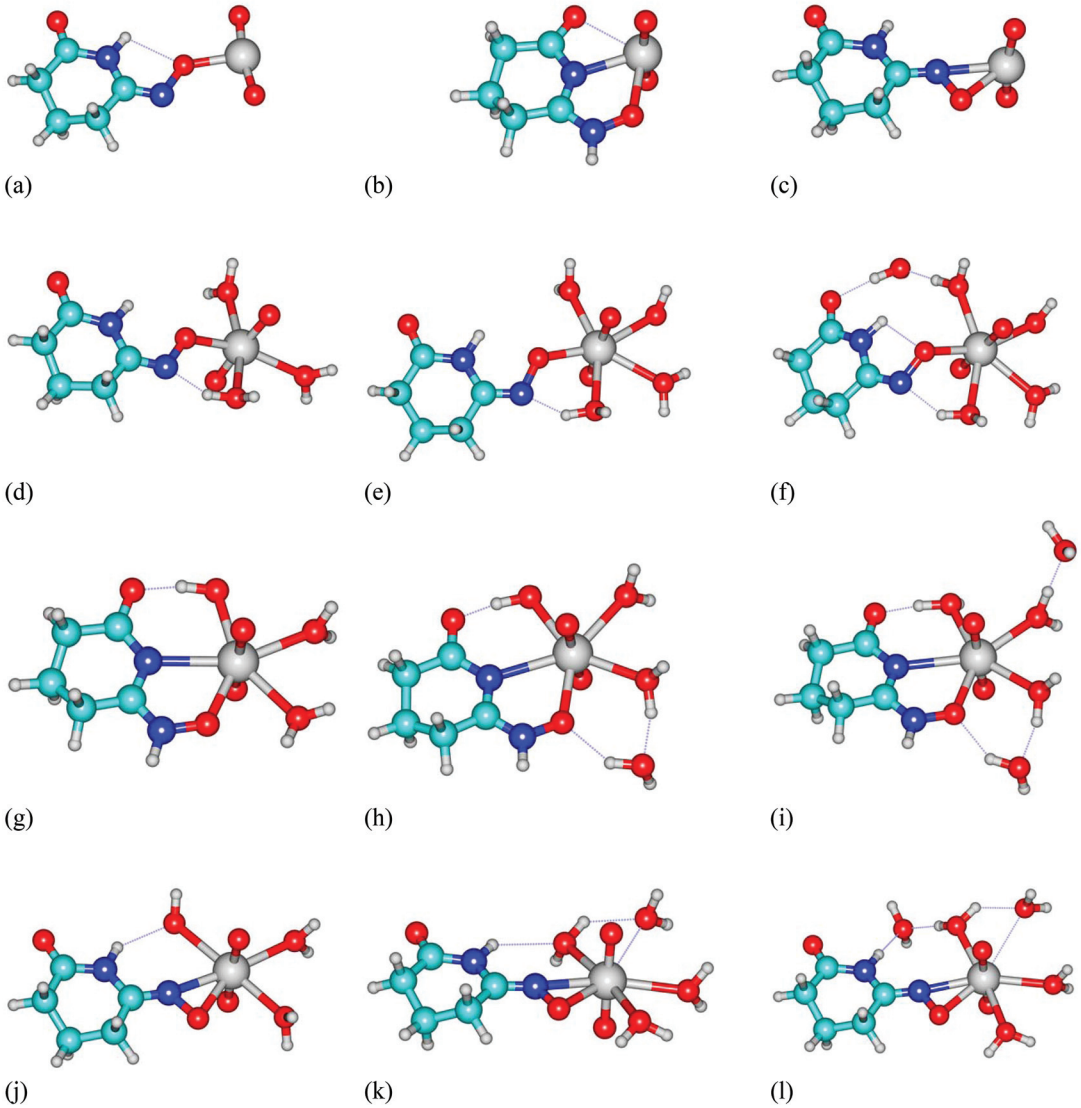


**Fig. 5** Optimized structures of the $[UO_2L^{III}(H_2O)_n{\cdot}m(H_2O)]^+$ complexes ($n$ = 0, 3, 4; $m$ = 0, 1, 2; $n + m$ = 0–5).

**Table 3** Selected bond distances (Å) for the optimized structures (from a to l) in the presence of PCM water. The U–$O_{water}$ bond distances represent the average values for all bonded water molecules (the standard deviations are in parentheses)

| | a | b | c | d | e | f | g | h | i | j | k | l |
|---|---|---|---|---|---|---|---|---|---|---|---|---|
| U–$O_{oxime}$ | 2.040 | 2.384 | 2.258 | 2.198 | 2.201 | 2.198 | 2.292 | 2.327 | 2.341 | 2.284 | 2.285 | 2.256 |
| U–$N_{oxime}$ | — | — | 2.371 | — | — | — | — | — | — | 2.335 | 2.356 | 2.411 |
| U–$N_{ring}$ | — | 2.381 | — | — | — | — | 2.633 | 2.673 | 2.684 | — | — | — |
| U–$O_{ring}$ | — | 2.890 | — | — | — | — | (3.757)[a] | (3.819)[a] | (3.279)[a] | — | — | — |
| U–$O_{water}$ | — | — | — | 2.51 (0.01) | 2.52 (0.03) | 2.53 (0.05) | 2.48 (0.04) | 2.47 (0.03) | 2.45 (0.02) | 2.56 (0.07) | 2.6 (0.1)[b] | 2.65 (0.04)[b] |

[a] These are unbound atoms, distances reported only for comparison with structure b. [b] In structures k and l one water dissociated during geometry optimization, with final distances of 2.80 Å (k) and 3.02 Å (l) (dotted U–$O_{water}$ bonds in Fig. 5).

Table 4 Free energies for the formation of the complexes (a to l in Fig. 5) in the gas phase and PCM water. The reactions considered are $[UO_2]^{2+} + (L^{III})^- \rightarrow [UO_2L^{III}]^+$ for the formation of a–c and $[UO_2(H_2O)_5]^{2+} + (L^{III})^- \rightarrow [UO_2L^{III}(H_2O)_n{\cdot}m(H_2O)]^+ + (5-n-m)H_2O$ for d–l

| | | | | $\Delta G$, kcal mol$^{-1}$ | |
|---|---|---|---|---|---|
| Coord. mode | Structure | $n$ | $5-n-m$ | Gas phase | PCM water |
| Monodentate | a | — | — | −351.3 | −38.4 |
| Bidentate | b | — | — | −392.2 | −37.5 |
| $\eta^2$ | c | — | — | −360.0 | −39.5 |
| Monodentate | d | 3 | 2 | −205.1 | −38.4 |
| | e | 4 | 1 | −210.1 | −37.8 |
| | f | 4 | 0 | −223.2 | −40.3 |
| Bidentate | g | 3 | 2 | −226.4 | −44.3 |
| | h | 3 | 1 | −229.9 | −46.2 |
| | i | 3 | 0 | −238.7 | −48.2 |
| $\eta^2$ | j | 3 | 2 | −214.6 | −39.9 |
| | k | 3 | 1 | −212.8 | −36.0 |
| | l | 3 | 0 | −223.5 | −38.1 |

$$[UO_2(H_2O)_5]^{2+} + (L^{III})^- \rightarrow [UO_2L^{III}(H_2O)_n \cdot m(H_2O)]^+ + (5-n-m)H_2O \quad (2)$$

Reaction (1) does not include the hydration effect, while reaction (2) takes into account the release/rearrangement of solvent molecules from the equatorial plane of the uranyl cation.

Structures a–c represent the minima obtained for the $(UO_2L^{III})^+$ complex with the three possible binding modes in Fig. 4 without any solvent molecules present. It is interesting to note that, differing from the hydrated structures (g–i), the uranium atom is able to weakly interact also with the carbonyl oxygen atom in structure b, as evidenced by the bond distances in Table 3. From a thermochemical point of view, the reactions for the formation of all structures have a markedly negative $\Delta G$ in the gas phase and PCM water (Table 4), primarily due to strongly exothermic interactions that largely compensate for the loss of entropy of the reagents. The computational results also show that the bidentate coordination is the most stable mode in the gas phase ($\Delta G$ (bi–mono) = −40.9 kcal mol$^{-1}$ and $\Delta G$ (bi–$\eta^2$) = −32.2 kcal mol$^{-1}$), but all three coordination modes are nearly equal in the free energy in PCM water: $\Delta G$ (bi–mono) = +0.9 kcal mol$^{-1}$ and $\Delta G$ (bi–$\eta^2$) = +2.0 kcal mol$^{-1}$. The $\eta^2$-coordination seems to be slightly more stable than the bi- and mono-dentate modes in PCM water.

When water molecules are introduced in the coordination sphere of the uranyl cation, a marked effect on the structures and relative stability of the U(VI) complexes is observed. For the structures d, e, g, and i in particular, the coordinated water molecules participate in the complexation by forming hydrogen bonds with the imino group and other N, O donor atoms (Fig. 5). The hydrogen bonding prevents the (weak) interaction between U and the carbonyl O that is present in structure b (Fig. 5). For the hydrated structures with the bidentate mode (g, h, and i), the average bond distances for U–$O_{oxime}$ and U–$N_{imino}$ are (2.27 ± 0.07) Å and (2.66 ± 0.03) Å, respectively. These bond distances are significantly different from the experimentally observed average distances of U–O and U–N in the Cambridge Structural Database (CSD), (2.40 ± 0.09) Å for U–O and (2.56 ± 0.10) Å for U–N, respectively.[21] In contrast, the U–$O_{oxime}$ and U–$N_{imino}$ distances in the U(VI)/$H_2L^I$ complex, 2.359 Å for U–$O_{oxime}$ and 2.516 Å for U–$N_{imino}$, are very close to those in the CSD.[40] Evidently, the deviations from the average experimentally observed distances are greater in the U(VI)/$HL^{III}$ complex than in the U(VI)/$H_2L^I$ complex. In other words, the U–$O_{oxime}$ bond is compressed and the U–$N_{imino}$ bond is stretched in the U(VI)/$HL^{III}$ complex, resulting in higher steric tension in the U(VI)/$HL^{III}$ complex than in the U(VI)/$H_2L^I$ complex. This means that the $HL^{III}$ ligand is structurally less complementary and accommodating than the $H_2L^I$ ligand for the formation of complexes with $UO_2^{2+}$. This poor structural match, along with the lower denticity of $HL^{III}$, is probably the structural origin of the much lower stability of the U(VI)/$HL^{III}$ complex than the U(VI)/$H_2L^I$ complex.

The water molecules in the second hydration shell can also form hydrogen bonds that increase the stability of the cyclic structures such as structures f, h, i, and l. With such hydrogen bonding, the more hydrated clusters with the monodentate mode and bidentate mode have higher stability in the gas phase: the stability of the monodentate structures follows the trend f > e > d, while the stability of the bidentate structures follows the trend i > h > g (Table 3). A different trend is observed for the $\eta^2$ structures (l > j > k), but in this case one water molecule is dissociated during the optimization process (Fig. 5 and Table 3), suggesting that the $\eta^2$ complexes should have only 3 waters in its first shell. The $\Delta G$ values are much less negative for all structures when the PCM solvation is introduced and the trends in the stability with increasing hydration are less systematic (for the monodentate mode: f > e ∼ d; for the bidentate mode: i > h > g; for the $\eta^2$ mode: j > l > k).

To help understand which coordination mode (mono-, bi-, or $\eta^2$) is the most probable one in the $(UO_2L^{III})^+$ complex, it is more meaningful to compare the energies of the structural isomers (mono-, bi-, or $\eta^2$) that follow the same desolvation scheme, *i.e.*, the same values of $(5-n-m)$ in reaction (2). The results in Table 3 show that for the hydrated structures optimized in PCM water, the most stable isomer is always the structure with the bidentate mode. For reaction (2) with the value of $(5-n-m) = 2$, the $\Delta G$ (kcal mol$^{-1}$) follows the trend: bi- (−44.3) < $\eta^2$- (−39.9) < mono- (−38.4). For reaction (2) with the value of $(5-n-m) = 1$, the $\Delta G$ (kcal mol$^{-1}$) follows the trend: bi- (−46.2) < mono- (−37.8) < $\eta^2$- (−36.0). For reaction (2) with the value of $(5-n-m) = 0$, the $\Delta G$ (kcal mol$^{-1}$) follows the trend: bi- (−48.2) < mono- (−40.3) < $\eta^2$- (−38.1). In brief, DFT computation suggests that the bidentate structure (Fig. 4a) is the most probable coordination mode in the $(UO_2L^{III})^+$ complex. Evidently, the formation of hydrogen bonding between a water molecule and the carbonyl oxygen atom in $HL^{III}$ stabilizes the bidentate coordination mode.

It is interesting to note that previous DFT computations indicate that the $\eta^2$- coordination mode is slightly more stable than the bidentate mode in the U(VI)/acetamidoxime

complex,[34] which seems to be contradictory to the computational results of the present study. However, the difference between the results of the previous and the present studies could actually be attributed to the difference in the structures between acetamidoxime and glutarimidoxioxime ($HL^{III}$). The carbonyl group, present in the latter ligand ($HL^{III}$) but absent in the former (acetamidoxime), could facilitate the formation of a hydrogen bond network which helps to stabilize the bidentate coordination mode in the $(UO_2L^{III})^+$ complex, as discussed in previous sections of this paper.

## Conclusion

The stability constant of a 1 : 1 complex between U(VI) and glutarimidoxioxime ($HL^{III}$), $(UO_2L^{III})^+$, has been determined by potentiometry. The complexation is too weak to effectively compete with the hydrolysis of U(VI) in slightly acidic to neutral solutions, or the complexation of U(VI) with carbonate anions in neutral to alkaline solutions. DFT calculations showed the importance of complex hydration in determining the structure and relative stability of the different possible coordination modes. Computational results suggested that a bidentate coordination mode, involving the oxime and imino groups, is stabilized by a hydrogen bond between water and the carbonyl group and is the most probable mode in the $(UO_2L^{III})^+$ complex.

Glutarimidoxioxime ($HL^{III}$) and two other amidoxime-related ligands, glutarimidedioxime ($H_2L^{I}$) and glutardiamidoxime ($H_2L^{II}$), represent the three possible functionalities that could be formed in the radiation-induced grafting process to prepare the sorbents for the extraction of uranium from seawater. The results from this study, in conjunction with those from previous studies, suggest that the conditions of the grafting process (*e.g.*, temperature, stoichiometric ratio of reactants) should be carefully selected and controlled to maximize the formation of glutarimidedioxime ($H_2L^{I}$), and probably glutardiamidoxime ($H_2L^{II}$) as well, but minimize the formation of glutarimidoxioxime ($HL^{III}$) because the binding strength of $HL^{III}$ with U(VI) is eight orders of magnitude lower than that of $H_2L^{I}$ and $H_2L^{II}$.

## Acknowledgements

The experimental work was supported by the Fuel Resources Program, Fuel Cycle Research and Development Program, Office of Nuclear Energy, the U.S. Department of Energy (USDOE). The computational work was supported by the Heavy Element Chemistry Program, Office of Basic Energy Science, Office of Science, USDOE under contract no. DE-AC02-05CH11231 at Lawrence Berkeley National Laboratory (LBNL). A.M. acknowledges CINECA (ISCRA "IscrC_M-2014" project) for computing time.

## Notes and references

1 J. Kim, C. Tsouris, R. T. Mayes, Y. Oyola, T. Saito, C. J. Janke, S. Dai, E. Schneider and D. Sachde, *Sep. Sci. Technol.*, 2013, **48**, 367.
2 OECD, *Uranium 2014: Resources, Production and Demand*, OECD NEA Publication 7209, 2014, p. 508.
3 R. V. Davies, J. Kennedy, R. W. McIlroy, R. Spence and K. M. Hill, *Nature*, 1964, **203**, 1110.
4 F. Endrizzi and L. Rao, *Chem. – Eur. J.*, 2014, **20**, 14499–14506.
5 J.-Y. Lee and J.-I. Yun, *Dalton Trans.*, 2013, **42**, 9862.
6 H. J. Schenk, L. Astheimer, E. G. Witte and K. Schwochau, *Sep. Sci. Technol.*, 1982, **17**, 1293.
7 L. Rao, *LBNL-4034, Recent International R & D Ativities in the Extraction of Uranium from Sea Water*, Lawrence Berkeley National Laboratory, Berkeley, California, USA, 2013.
8 G. Tian, S. J. Teat, Z. Zhang and L. Rao, *Dalton Trans.*, 2012, **41**, 11579.
9 G. Tian, S. J. Teat and L. Rao, *Dalton Trans.*, 2013, **42**, 5690.
10 C. W. Sill and H. E. Peterson, *Anal. Chem.*, 1947, **19**, 646.
11 P. Gans, A. Sabatini and A. Vacca, *Talanta*, 1996, **43**, 1739.
12 L. Alderighi, P. Gans, A. Ienco, D. Peters, A. Sabatini and A. Vacca, *Coord. Chem. Rev.*, 1999, **184**, 311.
13 P. L. Zanonato, P. Di Bernardo, A. Bismondo, G. Liu, X. Chen and L. Rao, *J. Am. Chem. Soc.*, 2004, **126**, 5515.
14 L. Rao, T. G. Srinivasan, A. Y. Garnov, P. Zanonato, B. Di Plinio and A. Bismondo, *Geochim. Cosmochim. Acta*, 2004, **68**, 4821.
15 R. Arnek, *Ark. Kemi*, 1970, **32**, 81.
16 A. D. Becke, *J. Chem. Phys.*, 1993, **98**, 1372.
17 C. T. Lee, W. T. Yang and R. G. Parr, *Phys. Rev. B: Condens. Matter*, 1988, **37**, 785.
18 P. Di Bernardo, P. L. Zanonato, F. Benetollo, A. Melchior, M. Tolazzi and L. Rao, *Inorg. Chem.*, 2012, **51**, 9045.
19 P. Di Bernardo, P. L. Zanonato, A. Bismondo, A. Melchior and M. Tolazzi, *Dalton Trans.*, 2009, 4236.
20 W. Kuchle, M. Dolg, H. Stoll and H. Preuss, *J. Chem. Phys.*, 1994, **100**, 7535.
21 J. Tomasi, B. Mennucci and R. Cammi, *Chem. Rev.*, 2005, **105**, 2999.
22 A. Melchior, E. Sánchez Marcos, R. R. Pappalardo and J. M. Martínez, *Theor. Chem. Acc.*, 2011, **128**, 627.
23 S. Del Piero, R. Fedele, A. Melchior, R. Portanova, M. Tolazzi and E. Zangrando, *Inorg. Chem.*, 2007, **46**, 1406.
24 P. Di Bernardo, A. Melchior, R. Portanova, M. Tolazzi and P. L. Zanonato, *Coord. Chem. Rev.*, 2008, **252**, 1270.
25 S. Del Piero, L. Ghezzi, A. Melchior, M. R. Tinè and M. Tolazzi, *Helv. Chim. Acta*, 2005, **88**, 839.
26 A. Melchior, E. Peralta, M. Valiente, C. Tavagnacco, F. Endrizzi and M. Tolazzi, *Dalton Trans.*, 2013, **42**, 6074.
27 S. Del Piero, R. Fedele, A. Melchior, R. Portanova, M. Tolazzi and E. Zangrando, *Inorg. Chem.*, 2007, **46**, 1406.
28 L. Cavallo, S. Del Piero, J.-M. Ducéré, R. Fedele, A. Melchior, G. Morini, F. Piemontesi and M. Tolazzi, *J. Phys. Chem. C*, 2007, **111**, 4412.

29 R. L. Martin, P. J. Hay and L. R. Pratt, *J. Phys. Chem. A*, 1998, **102**, 3565.
30 M. J. Frisch, *et al.*, *Gaussian 09, Revis. A.02*, 2009 (a complete list of co-authors is provided in the ESI†).
31 R. Guillaumont, T. Fanghanel, J. Fuger, I. Grenthe, V. Neck, D. A. Palmer and M. H. Rand, *Update on the chemical thermodynamics of uranium, neptunium, plutonium, americium and technetium*, ed. F. J. Mompean, M. Illemassene, C. Domenech-Orti and B. K. Said, Elsevier B. V., Amsterdam, 2003, p. 964.
32 W. Hummel, G. Anderegg, I. Puigdomenech, L. Rao and O. Tochiyama, *Chemical Thermodynamics of Compounds and Complexes of U, Np, Pu, Am, Tc, Se, Ni and Zr with Selected Organic Ligands*, ed. F. J. Mompean, M. Illemassene and J. Perrone, OECD Nuclear Energy Agency, Data Bank, Issy-les-Moulineaux, France, 2005, p. 1088.
33 L. Ciavatta, *Ann. Chim.*, 1980, **70**, 551.
34 S. Vukovic, L. A. Watson, S. O. Kang, R. Custelcean and B. P. Hay, *Inorg. Chem.*, 2012, **51**, 3855.
35 C.-Z. Wang, J.-H. Lan, Q.-Y. Wu, Q. Luo, Y.-L. Zhao, X.-K. Wang, Z.-F. Chai and W.-Q. Shi, *Inorg. Chem.*, 2014, **53**, 9466.
36 T. Hirotsu, S. Katoh, K. Sugasaka, M. Seno and T. Itagaki, *J. Chem. Soc., Dalton Trans.*, 1986, 1609.
37 P. S. Barber, S. P. Kelley and R. D. Rogers, *RSC Adv.*, 2012, **2**, 8526.
38 S. P. Kelley, P. S. Barber, P. H. K. Mullins and R. D. Rogers, *Chem. Commun.*, 2014, **50**, 12504.
39 I. Kron, S. L. Marshall, P. M. May, G. Hefter and E. Koenigsberger, *Monatsh. Chem.*, 1995, **126**, 819.
40 X. Sun, G. Tian, C. Xu, L. Rao, S. Vukovic, S. O. Kang and B. P. Hay, *Dalton Trans.*, 2014, **43**, 551.